Satellite Image Resolution Enhancement Using Dual-Tree Complex Wavelet Transform and Nonlocal Means

Muhammad Zafar Iqbal, Abdul Ghafoor, and Adil Masood Siddiqui

***Abstract*—Resolution enhancement (RE) schemes (which are not based on wavelets) suffer from the drawback of losing high-frequency contents (which results in blurring). The discrete-wavelet-transform-based (DWT) RE scheme generates artifacts (due to a DWT shift-variant property). A wavelet-domain approach based on dual-tree complex wavelet transform (DT-CWT) and nonlocal means (NLM) is proposed for RE of the satellite images. A satellite input image is decomposed by DT-CWT (which is nearly shift invariant) to obtain high-frequency subbands. The high-frequency subbands and the low-resolution (LR) input image are interpolated using the Lanczos interpolator. The high-frequency subbands are passed through an NLM filter to cater for the artifacts generated by DT-CWT (despite of its nearly shift invariance). The filtered high-frequency subbands and the LR input image are combined using inverse DT-CWT to obtain a resolution-enhanced image. Objective and subjective analyses reveal superiority of the proposed technique over the conventional and state-of-the-art RE techniques.**

***Index Terms*—Dual-tree complex wavelet transform (DT-CWT), Lanczos interpolation, resolution enhancement (RE), shift variant.**

I. Introduction

RESOLUTION (spatial, spectral, and temporal) is the limiting factor for the utilization of remote sensing data (satellite imaging, etc.). Spatial and spectral resolutions of satellite images (unprocessed) are related (a high spatial resolution is associated with a low spectral resolution and vice versa) with each other [1]. Therefore, spectral, as well as spatial, resolution enhancement (RE) is desirable.

Interpolation has been widely used for RE [2], [3]. Commonly used interpolation techniques are based on nearest neighbors (include nearest neighbor, bilinear, bicubic, and Lanczos). The Lanczos interpolation (windowed form of a sinc filter) is superior than its counterparts (including nearest neighbor, bilinear, and bicubic) due to increased ability to detect edges and linear features. It also offers the best compromise in terms of reduction of aliasing, sharpness, and ringing [4].

Methods based on vector-valued image regularization with partial differential equations (VVIR-PDE) [5] and inpainting and zooming using sparse representations [6] are now state of the art in the field (mostly applied for image inpainting but can be also seen as interpolation).

RE schemes (which are not based on wavelets) suffer from the drawback of losing high-frequency contents (which results in blurring).

RE in the wavelet domain is a new research area, and recently, many algorithms [discrete wavelet transform (DWT) [7], stationary wavelet transform (SWT) [8], and dual-tree complex wavelet transform (DT-CWT) [9] have been proposed [7]–[11]. An RE scheme was proposed in [9] using DT-CWT and bicubic interpolations, and results were compared (shown superior) with the conventional schemes (i.e., nearest neighbor, bilinear, and bicubic interpolations and wavelet zero padding). More recently, in [7], a scheme based on DWT and bicubic interpolation was proposed, and results were compared with the conventional schemes and the state-of-art schemes (wavelet zero padding and cyclic spinning [12] and DT-CWT [9]). Note that, DWT is shift variant, which causes artifacts in the RE image, and has a lack of directionality; however, DT-CWT is almost shift and rotation invariant [13].

DWT-based RE schemes generate artifacts (due to DWT shift-variant property).

In this letter, a DT-CWT-based nonlocal-means-based RE (DT-CWT-NLM-RE) technique is proposed, using the DT-CWT, Lanczos interpolation, and NLM. Note that DT-CWT is nearly shift invariant and directional selective. Moreover, DT-CWT preserved the usual properties of perfect reconstruction with well-balanced frequency responses [13], [14]. Consequentially, DT-CWT gives promising results after the modification of the wavelet coefficients and provides less artifacts, as compared with traditional DWT. Since the Lanczos filter offer less aliasing, sharpness, and minimal ringing, therefore, it a good choice for RE. NLM filtering [15] is used to further enhance the performance of DT-CWT-NLM-RE by reducing the artifacts. The results (for spatial RE of optical images) are compared with the best performing techniques [5], [7]–[9].

II. Preliminaries

A. NLM Filtering

The NLM filter (an extension of neighborhood filtering algorithms) is based on the assumption that image content is likely to repeat itself within some neighborhood (in the image) [15] and in neighboring frames [16]. It computes denoised pixel $x(p, q)$ by the weighted sum of the surrounding pixels of

Manuscript received February 16, 2012; revised April 28, 2012 and June 10, 2012; accepted July 6, 2012. Date of publication August 24, 2012; date of current version November 24, 2012.

The authors are with the Department of Electrical Engineering, Military College of Signals, National University of Sciences and Technology, Islamabad H-12, Pakistan (e-mail: mzafar.iqbal@mcs.edu.pk; abdulghafoor-mcs@nust.edu.pk; dradil@mcs.edu.pk).

Color versions of one or more of the figures in this paper are available online at http://ieeexplore.ieee.org.

Digital Object Identifier 10.1109/LGRS.2012.2208616

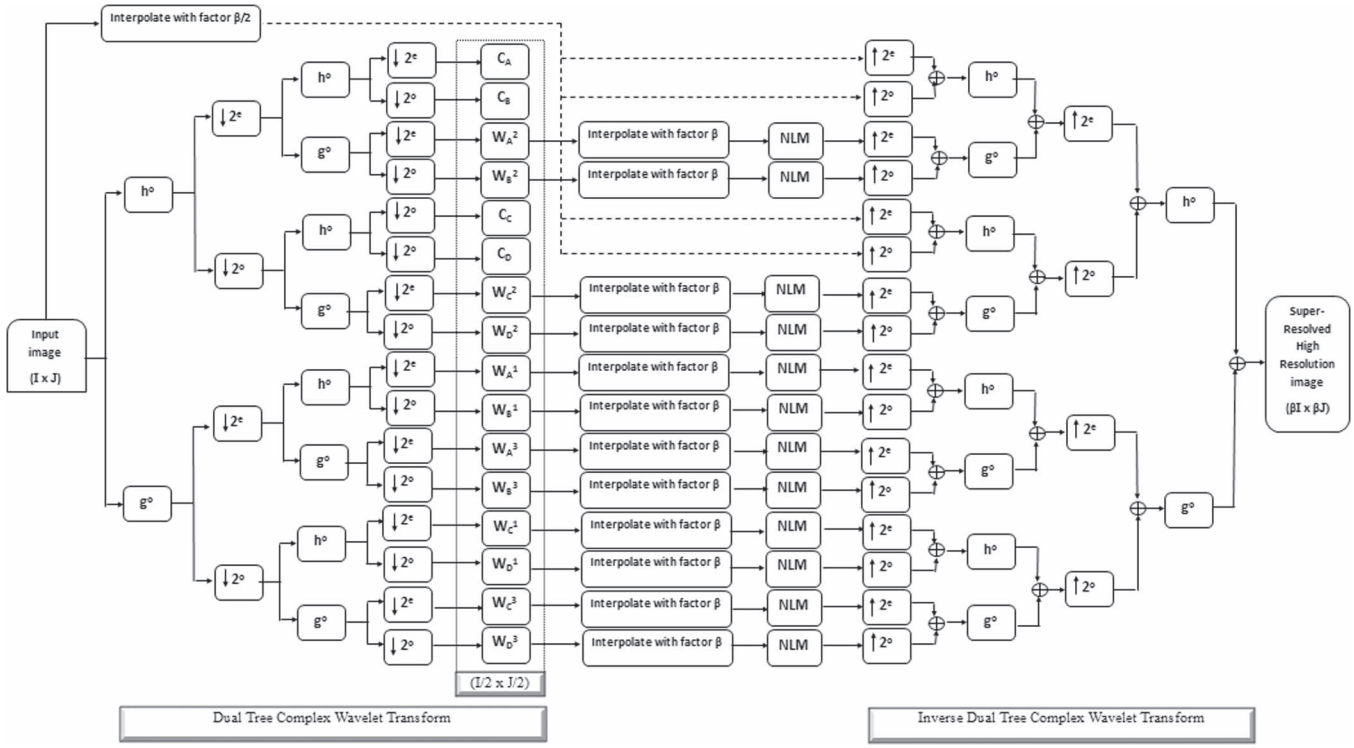

Fig. 1. Block diagram of the proposed DT-CWT-RE algorithm.

$Y(p,q)$ (within frame and in the neighboring frames) [16]. This feature provides a way to estimate the pixel value from noise-contaminated images. In a 3-D NLM algorithm, the estimate of a pixel at position (p,q) is

$$x(p,q) = \frac{\sum_{m=1}^{M} \sum_{(r,s)\in N(p,q)} Y_m(r,s) K_m(r,s)}{\sum_{m=1}^{M} \sum_{(r,s)\in N(p,q)} K_m(r,s)} \tag{1}$$

where m is the frame index, and N represents the neighborhood of the pixel at location (p,q). K values are the filter weights, i.e.,

$$K(r,s) = \exp\left\{-\frac{\|V(p,q) - V(r,s)\|_2^2}{2\sigma^2}\right\} \times f\left(\sqrt{(p-r)^2 + (q-s)^2 + (m-1)^2}\right) \tag{2}$$

where V is the window [usually a square window centered at the pixels $Y(p,q)$ and $Y(r,s)$] of pixel values from a geometric neighborhood of pixels $Y(p,q)$ and $Y(r,s)$, σ is the filter coefficient, and $f(.)$ is a geometric distance function. K is inversely proportional to the distance between $Y(p,q)$ and $Y(r,s)$.

B. NLM-RE

RE is achieved by modifying NLM with the following model [17]:

$$L_m = IJQX + n \tag{3}$$

where L_m is the vectorized low-resolution (LR) frame, I is the decimation operator, J is the blurring matrix, Q is the warping matrix, X is the vectorized high-resolution (HR) image, and n denotes the Gaussian white noise. The aim is to restore X from a series of L. Penalty function ϵ is defined as

$$\epsilon^2 = \frac{1}{2}\sum_{m=1}^{M} \|IJQx - Y_m\|_2^2 + \lambda R(x) \tag{4}$$

where R is a regularization term, λ is the scale coefficient, x is the targeted image, and Y_m is the LR input image. In [17], the total variation kernel is chosen to replace R, acting as an image deblurring kernel. To simplify the algorithm, a separation of the problem in (4) is done by minimizing

$$\epsilon_{\text{fusion}}^2(Z) = \frac{1}{2}\sum_{m=1}^{M} (IQZ - L_m)^T O_m (IQZ - L_m) \tag{5}$$

where Z is the blurred version of the targeted image, and O_m is the weight matrix, followed by minimizing a deblurring equation [11], i.e.,

$$\epsilon_{\text{RE}}^2(X) = \|JX - Z\|_2^2 + \lambda R(Z). \tag{6}$$

A pixelwise solution of (5) can be obtained as

$$\hat{z} = \frac{\sum_{m=1}^{M} \sum_{(r,s)\in N(p,q)} Y_m^r(r,s) K_m^r(r,s)}{\sum_{m=1}^{M} \sum_{(r,s)\in N(p,q)} K_m^r(r,s)} \tag{7}$$

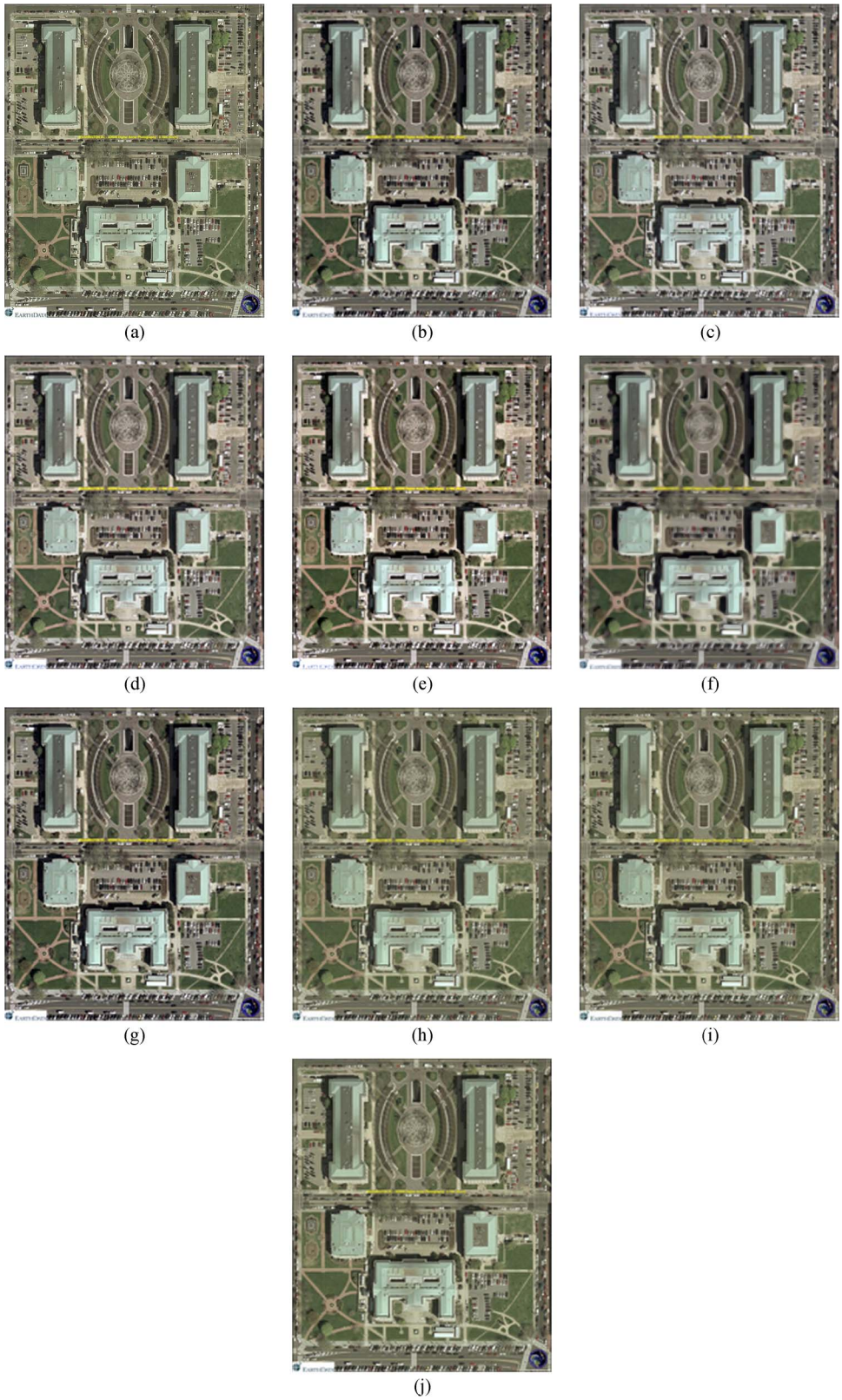

Fig. 2. (a) Original "Washington DC" image. (b) Input image. (c) SWT-RE. (d) DWT-RE. (e) SWT-DWT-RE. (f) VVIR-PDE-RE. (g) Lanczos Interpolation. (h) DT-CWT-RE. (i) Proposed DT-CWT-RE. (j) Proposed DT-CWT-NLM-RE.

where the superscript r refers to the HR coordinate. Instead of estimating the target pixel position in nearby frames, this algorithm considers all possible positions where the pixel may appear; therefore, motion estimation is avoided [11]. Equation (7) apparently resembles (1), but (7) has some differences as compared with (1). The weight estimation in (2) should be modified because K's corresponding matrix O has to be of the same size as the HR image. Therefore, a simple upscaling

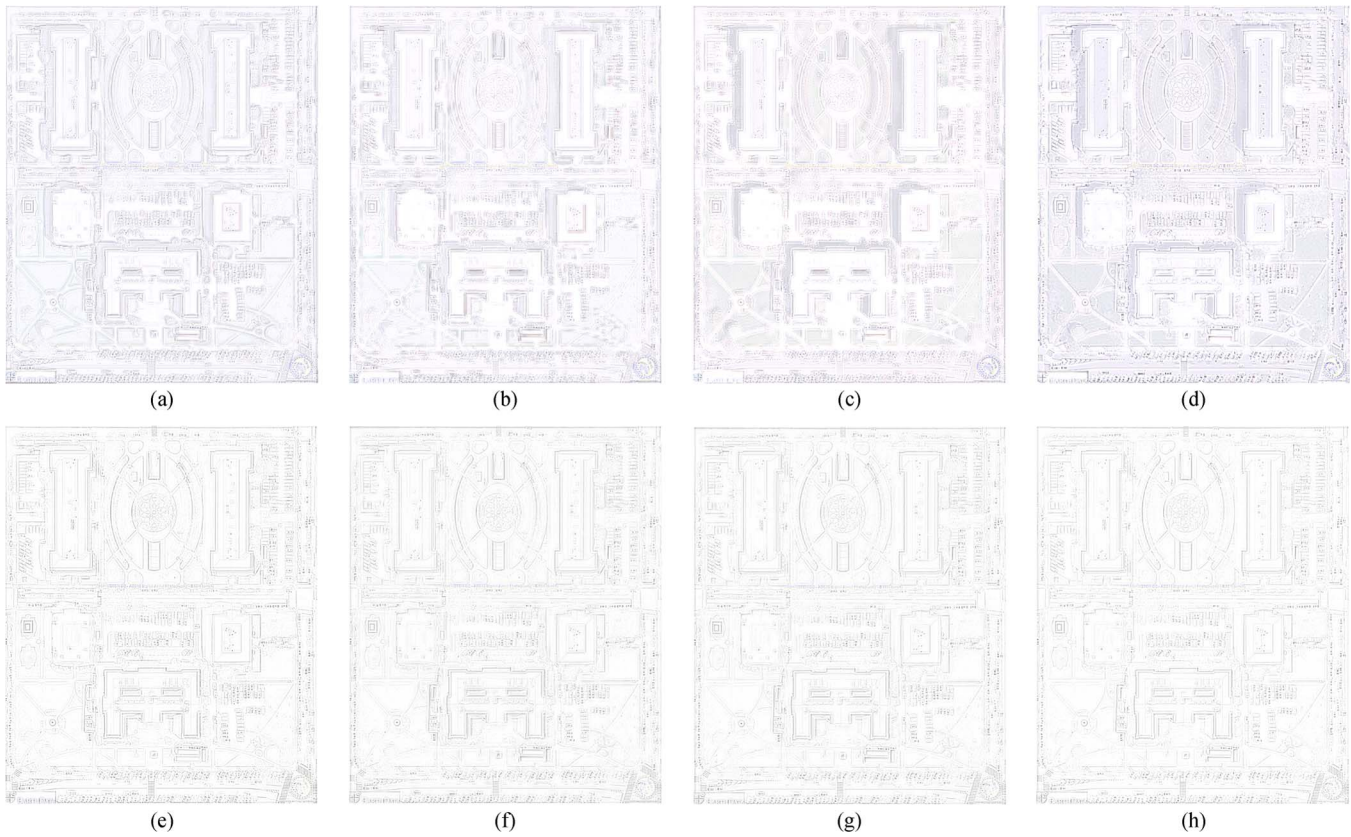

Fig. 3. Negative of the difference images for (a) SWT-RE, (b) DWT-RE (c) SWT-DWT-RE, (d) VVIR-PDE-RE, (e) Lanczos-RE, (f) DT-CWT-RE, (g) Proposed DT-CWT-RE, and (h) Proposed DT-CWT-NLM-RE.

process to patch V is needed before computing K. The total number of pixel Y in (7) should be equal to the number of weights K. Thus, a zero-padding interpolation is applied to L before fusing the images [11].

III. Proposed Technique

In the proposed algorithm (DT-CWT-NLM-RE), we decompose the LR input image (for the multichannel case, each channel is separately treated) in different subbands (i.e., C_i and W_i^j, where $i \in \{A, B, C, D\}$ and $j \in \{1, 2, 3\}$) by using DT-CWT, as shown in Fig. 1. C_i values are the image coefficient subbands, and W_i^j are the wavelet coefficient subbands. The subscripts A, B, C, and D represent the coefficients at the even-row and even-column index, the odd-row and even-column index, the even-row and odd-column index and the odd-row and odd-column index, respectively, whereas h and g represent the low-pass and high-pass filters, respectively. The superscript e and o represent the even and odd indices, respectively.

W_i^j values are interpolated by factor β using the Lanczos interpolation (having good approximation capabilities) and combined with the $\beta/2$-interpolated LR input image. Since C_i contains low-pass-filtered image of the LR input image, therefore, high-frequency information is lost. To cater for it, we have used the LR input image instead of C_i.

Although the DT-CWT is almost shift invariant [14], however, it may produce artifacts after the interpolation of W_i^j. Therefore, to cater for these artifacts, NLM filtering is used. All interpolated W_i^j values are passed through the NLM filter. Then, we apply the inverse DT-CWT to these filtered subbands along with the interpolated LR input image to reconstruct the HR image. The results presented show that the proposed DT-CWT-NLM-RE algorithm performs better than the existing wavelet-domain RE algorithms in terms of the peak-signal-to-noise ratio (PSNR), the MSE, and the Q-index [18].

IV. Results and Discussion

To ascertain the effectiveness of the proposed DT-CWT-NLM-RE algorithm over other wavelet-domain RE techniques, different LR optical images obtained from the Satellite Imaging Corporation webpage [1] were tested. The image of Washington DC ADS40 Orthorectified Digital Aerial Photography -0.15 m is chosen here for comparison with existing RE techniques. Note that the input LR image has been obtained by downsampling the original HR by a factor of 4. Fig. 2 shows the original "Washington DC" image, the downsampled input image, and the images obtained using SWT-RE [8], DWT-RE [7], SWT-DWT-RE [8], VVIR-PDE-RE [4], Lanczos interpolation, DT-CWT-RE [9], proposed DT-CWT-RE, and proposed DT-CWT-NLM-RE. Fig. 3 shows the difference of the original image and images obtained using SWT-RE [8], DWT-RE [7], SWT-DWT-RE [8], VVIR-PDE-RE [5], Lanczos-RE, DT-CWT-RE [9], proposed DT-CWT-RE, and proposed DT-CWT-NLM-RE. It can be seen that the results of the proposed

TABLE I
COMPARISON OF THE EXISTING AND PROPOSED TECHNIQUES FOR THE "WASHINGTON DC" IMAGE

Algorithm	MSE	PSNR(dB)	Q-index
SWT-RE [8]	0.0464	13.3332	0.9942
DWT-RE [7]	0.0419	13.7802	0.9901
SWT-DWT-RE [8]	0.0335	14.7527	0.9660
VVIR-PDE-RE [5]	0.0269	15.6970	0.9642
Lanczos-RE	0.0253	15.9770	0.9614
DT-CWT-RE [9]	0.0242	16.1576	0.9986
Proposed DT-CWT-RE	0.0215	16.6658	0.9986
Proposed DT-CWT-NLM-RE	0.0174	17.5895	0.9999

algorithm DT-CWT-NLM-RE are much better than the RE images obtained using other techniques. Table I shows that the proposed techniques provide improved results in terms of MSE, PSNR, and Q-index [18], as compared with other techniques. It is clear that the proposed DT-CWT-RE and DT-CWT-NLM-RE schemes outperform SWT, DWT, SWT-DWT-RE, VVIR-PDE-RE, and DT-CWT-RE techniques qualitatively and quantitatively.

V. CONCLUSION

An RE technique based on DT-CWT and an NLM filter has been proposed. The technique decomposes the LR input image using DT-CWT. Wavelet coefficients and the LR input image were interpolated using the Lanczos interpolator. DT-CWT is used since it is nearly shift invariant and generates less artifacts, as compared with DWT. NLM filtering is used to overcome the artifacts generated by DT-CWT and to further enhance the performance of the proposed technique in terms of MSE, PSNR, and Q-index. Simulation results highlight the superior performance of proposed techniques.

ACKNOWLEDGMENT

The authors would like to thank Satellite Imaging Corporation for providing satellite images for research purpose.

REFERENCES

[1] [Online].Available:http://www.satimagingcorp.com/
[2] Y. Piao, I. Shin, and H. W. Park, "Image resolution enhancement using inter-subband correlation in wavelet domain," in *Proc. Int. Conf. Image Process.*, San Antonio, TX, 2007, pp. I-445–I-448.
[3] C. B. Atkins, C. A. Bouman, and J. P. Allebach, "Optimal image scaling using pixel classification," in *Proc. Int. Conf. Image Process.*, Oct. 7–10, 2001, pp. 864–867.
[4] A. S. Glassner, K. Turkowski, and S. Gabriel, "Filters for common resampling tasks," in *Graphics Gems*. New York: Academic, 1990, pp. 147–165.
[5] D. Tschumperle and R. Deriche, "Vector-valued image regularization with PDE's: A common framework for different applications," *IEEE Trans. Pattern Anal. Mach. Intell.*, vol. 27, no. 4, pp. 506–517, Apr. 2005.
[6] M. J. Fadili, J. Starck, and F. Murtagh, "Inpainting and zooming using sparse representations," *Comput. J.*, vol. 52, no. 1, pp. 64–79, Jan. 2009.
[7] H. Demirel and G. Anbarjafari, "Discrete wavelet transform-based satellite image resolution enhancement," *IEEE Trans. Geosci. Remote Sens.*, vol. 49, no. 6, pp. 1997–2004, Jun. 2011.
[8] H. Demirel and G. Anbarjafari, "Image resolution enhancement by using discrete and stationary wavelet decomposition," *IEEE Trans. Image Process.*, vol. 20, no. 5, pp. 1458–1460, May 2011.
[9] H. Demirel and G. Anbarjafari, "Satellite image resolution enhancement using complex wavelet transform," *IEEE Geosci. Remote Sens. Lett.*, vol. 7, no. 1, pp. 123–126, Jan. 2010.
[10] H. Demirel and G. Anbarjafari, "Image super resolution based on interpolation of wavelet domain high frequency subbands and the spatial domain input image," *ETRI J.*, vol. 32, no. 3, pp. 390–394, Jan. 2010.
[11] H. Zheng, A. Bouzerdoum, and S. L. Phung, "Wavelet based non-local-means super-resolution for video sequences," in *Proc. IEEE 17th Int. Conf. Image Process.*, Hong Kong, Sep. 26–29, 2010, pp. 2817–2820.
[12] A. Gambardella and M. Migliaccio, "On the superresolution of microwave scanning radiometer measurements," *IEEE Geosci. Remote Sens. Lett.*, vol. 5, no. 4, pp. 796–800, Oct. 2008.
[13] I. W. Selesnick, R. G. Baraniuk, and N. G. Kingsbur, "The dual-tree complex wavelet transform," *IEEE Signal Prcess. Mag.*, vol. 22, no. 6, pp. 123–151, Nov. 2005.
[14] J. L. Starck, F. Murtagh, and J. M. Fadili, *Sparse Image and Signal Processing: Wavelets, Curvelets, Morphological Diversity*. Cambridge, U.K.: Cambridge Univ. Press, 2010.
[15] A. Buades, B. Coll, and J. M. Morel, "A review of image denoising algorithms, with a new one," *Multisc. Model. Simul.*, vol. 4, no. 2, pp. 490–530, 2005.
[16] A. Buades, B. Coll, and J. M. Morel, "Denoising image sequences does not require motion estimation," in *Proc. IEEE Conf. Audio, Video Signal Based Surv.*, 2005, pp. 70–74.
[17] M. Protter, M. Elad, H. Takeda, and P. Milanfar, "Generalizing the nonlocal-means to super-resolution reconstruction," *IEEE Trans. Image Process.*, vol. 18, no. 1, pp. 36–51, Jan. 2009.
[18] Z. Wang and A. C. Bovik, "A universal image quality index," *IEEE Signal Process. Lett.*, vol. 9, no. 3, pp. 81–84, Mar. 2002.